JP 3.5

EXPERIMENTALLY MEASURED SCATTERING PROPERTIES OF PLATE AND COLUMN ICE CRYSTALS

Brian Barkey* and K. N. Liou
University of California, Los Angeles, Los Angeles, Calif.
Matt Bailey, and John Hallet
Desert Research Institute, University of Nevada, Nevada

1. INTRODUCTION

This paper presents the results of an ongoing experimental research effort to measure the single scattering properties of ice crystals. The highly anisotropic scattering properties of the non-spherical particles of which ice clouds, i.e., cirrus, are composed of are important in understanding the global radiation budget (Liou 1986) and for remote sensing applications (Rolland et al. 2000). Several other experimental investigations into the scattering properties of ice crystals have been previously performed both *in situ*, (e.g., Oschepkov et al. 2000) and in the laboratory setting (e.g., Sassen and Liou 1979). Because the cloud chamber at the Desert Research Institute can produce clouds composed of ice particles which are roughly the same in size and morphology, a study of scattering properties as a function of particle habit is possible.

A brief description of the cloud chamber and polar nephelometer is presented, followed by the measurements of ice particles composed of primarily columns, and another cloud composed of primarily plates. These results are compared to theoretical expectations based on the observed microphysics of the ice particles.

2. POLAR NEPHELOMETER

The polar nephelometer (Fig. 1) previously described in Barkey and Liou (2000) consists of an array of 33 discrete fiber optic coupled photo diode detectors arranged in a two-dimensional (2D) plane to detect the scattered light intensities between the angles of 5° and 175°. A light beam highly polarized parallel to the scattering plane at a wavelength of 0.67 µm from a 35 milliwatt laser diode is collimated into an elliptical beam, approximately 4 mm tall and 2 mm wide. This beam is then directed across the plane of detection to intercept particles which are channeled into the center of the detector array by an aluminum tube with an inside diameter of 3 mm.

The particles are removed out of the bottom of the instrument by another aluminum tube with an inside diameter of 5 mm. The gap between the sample tubes is about 8 mm. Two light absorbers are placed above and below the scattering plane to reduce the effect of secondary reflections within the instrument. The instrument has a linear response correct to within 1% except at lower intensity levels, where instrument noise that produces an error of 10% defines a dynamic range of about three decades. Although a single measurement of the light scattered into the array takes less than 0.05 seconds, operationally only about 8 measurements per second can be transmitted to an external computer for storage.

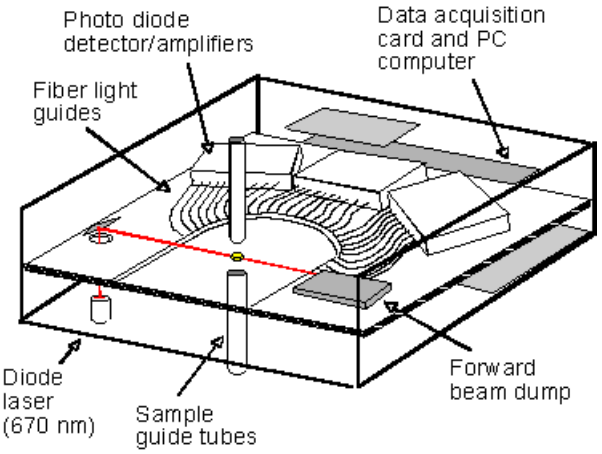

Fig. 1. Polar Nephelometer

3. CLOUD CHAMBER

The cloud chamber, which is an upgraded version of the chamber used by Arnott et al. (1995), consists of an insulated and refrigerated column about 4 m tall and 0.3 m in diameter positioned above a larger cold chamber. Several thermocouples are placed along the length of the growth column. Water droplets from an ultrasonic humidifier fall and cool to the desired temperature in the upper column, some of which are nucleated by a wire spring, which is continuously cooled by liquid nitrogen and presented to the ice cloud by a system

*Corresponding author address: Brian Barkey, Department of Atmospheric Sciences, University of California, Los Angeles, Los Angeles, Calif. 90095-1565; e-mail: brian_barkey@juno.com

of pulleys and a slowly rotating electric motor.

The ice crystal habit is mainly controlled by the temperature at which they are allowed to grow after nucleation. The nucleated ice crystals continue to grow at the expense of water droplets as they fall through the growth column and into the lower cold chamber where the polar nephelometer is placed. The ice crystal properties are monitored by a cloudscope positioned about 20 cm from the nephelometer sample inlet. The cloudscope is a video microscope that observes the particles which fall onto a sapphire window.

4. EXPERIMENTAL RESULTS

Because of the small volume in which the laser beam intersects the particles, it is anticipated that the effect of multiple scattering on the nephelometer measurement can be neglected. The intensity of the light scattered into the 2D plane where the fiber light guides are positioned depends on the number of particles in the scattering volume, and the size, shape and orientation of these particles. These parameters vary considerably during experiments which causes the intensity of the measured results to vary widely from one measurement to the next as shown in Fig. 2. The standard deviation of the measured intensity at each angle for measurements that are above the low intensity noise level comprises 40% to 70% of the measured mean when determined using the results of a single cloud event of more than 100 measurements. For these reasons, we decided to average the scattering patterns over several hundred measurements where it is assumed that the ice cloud habits and concentration remain constant. About 190 measurements are needed to reduce the standard error of the mean at each measured angle to less than 5%. Thus, the average scattering pattern corresponds to an ice crystal with the scattering properties of all the particles that existed during the time period of the experiment.

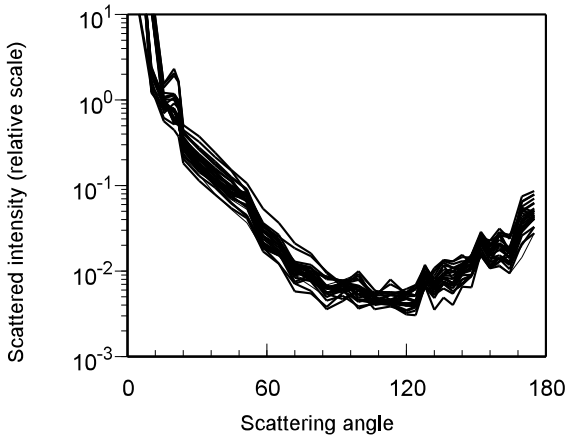

Fig.2. Several 2D scattering measurements of ice crystals indicative of changing experimental conditions.

Shown at the top of Fig. 3 is a cloudscope video image when the crystal habit of the cloud consisted of predominantly plates and short columns grown at a temperature of about -6° C. The vertical white stripe in this image is due to glare from the cloudscope light source. The particles have an average maximum dimension of 17 μm ± 0.5 μm and are composed of mostly plates (≈ 60%) and short columns. The average aspect ratio (or $L/2a$, where a is the radius of the hexagonal face and L is the length of the column or the thickness of a plate) is about 0.8. Because plate thickness could not be

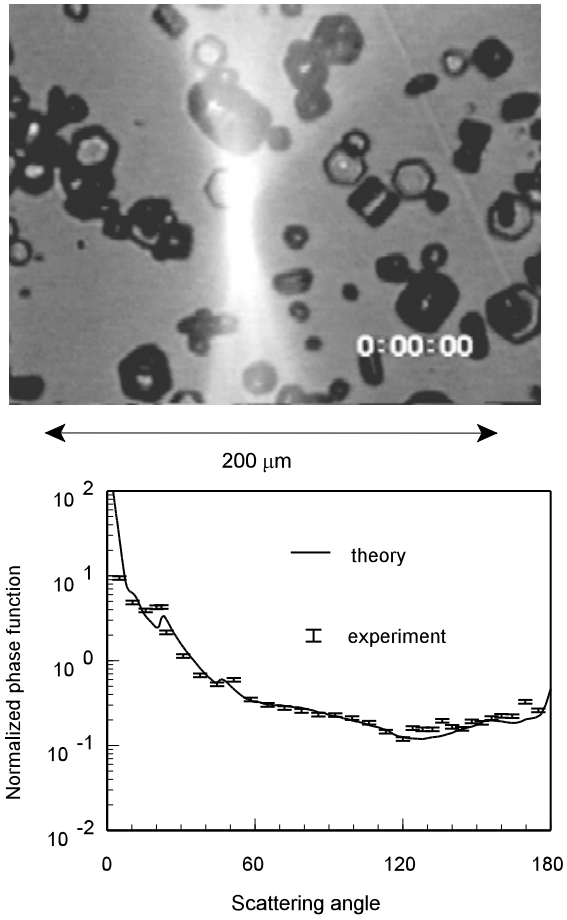

Fig. 3. Cloudscope image of plates present when the scattering properties shown below were measured by the nephelometer. These results are fitted to the theoretical expectation.

directly measured from these images, the plate thickness, h, is determined from, $h = 0.014\ d^{0.474}$, where d is plate diameter between 10 μm and 3000 μm from Pruppacher and Klett (1980). The experimentally measured scattering properties from the average of 189 measurements taken over a period of about three minutes are fitted to the theoretical expectation that is based on the observed particle microphysics. The error bars correspond to the 5% standard error of the mean.

Fig. 4 is similar to Fig. 3 except that it involves a cloud event when mostly hollow columns were seen by the cloud scope. The 26 particles counted from this image consist of mostly hollow columns with an average aspect ratio of about 2.1 and an average maximum dimension of about 36 μm ± 0.5 μm. Regular columns, trigonal shapes, and plates are also seen. The experimental result is the average of 511 measurements taken over a period of approximately 4.5 minutes. The standard error of the mean for this result produces about 3% of error.

Normalized phase functions for simple hexagons and hollow columns calculated using geometric optics methods (Takano and Liou 1989) with various aspect ratios approximately corresponding to the measured crystal sizes are combined using the extinction cross section determined from the measured crystal size and the counted population to weight the scattering contributions of each particle. For randomly oriented simple hexagonal particles, the extinction cross section (C_e) is approximated with:

$$C_e = \frac{3a^2}{2}\left(\sqrt{3} + 4\left[\frac{L}{2a}\right]\right), \qquad (1)$$

where particle length (L) and radius (a) are measured directly from the images or calculated as described above (Takano and Liou 1989). In Fig. 3 approximately 80% of the particles were assumed to have rough surfaces to account for the surface features that are seen on some of the larger plates in the cloudscope image. Surface roughness was incorporated in the phase functions by random perturbations of the crystal surface (Yang and Liou 1996). In Fig. 4, about 10% of the phase functions used to produce the theoretical values are based on the hollow column habit. The other particles are simple columns and plates, of which 80% have rough surfaces.

Overall, the experimental results closely follow the theoretical values. Both the 22° and 46° halo intensity features are clearly displayed, although there is less intensity at the 46° feature for the hollow column case. This is expected as the 46° halo feature is produced by refraction through a 90° prism, which is more prevalent in plates than in columns. For both results, a large percentage of the theoretical expectations required particles with rough surfaces to provide a reasonable fit to the experimental results, yet there is more measured light scattered into the angles between 10° and 20° than expected. This is most likely due to surface features on the particles which cannot be seen on the cloudscope images due to the low resolution of the video camera and/or smaller particles not seen by the cloud scope. For particles collected using gravitational sedimentation, a cut off at 7 μm has been estimated for an automated replicator system previously used in this chamber (Arnott et al. 1995).

Note that the expectation did not include several particle habits, including the trigonals mentioned earlier, the end features seen on some of the columns of Fig. 4, and the particles which are too small, or irregular to classify as seen in Fig. 3. The measured intensity between 160° and 175° of Fig. 4 is much higher than expected which is most likely

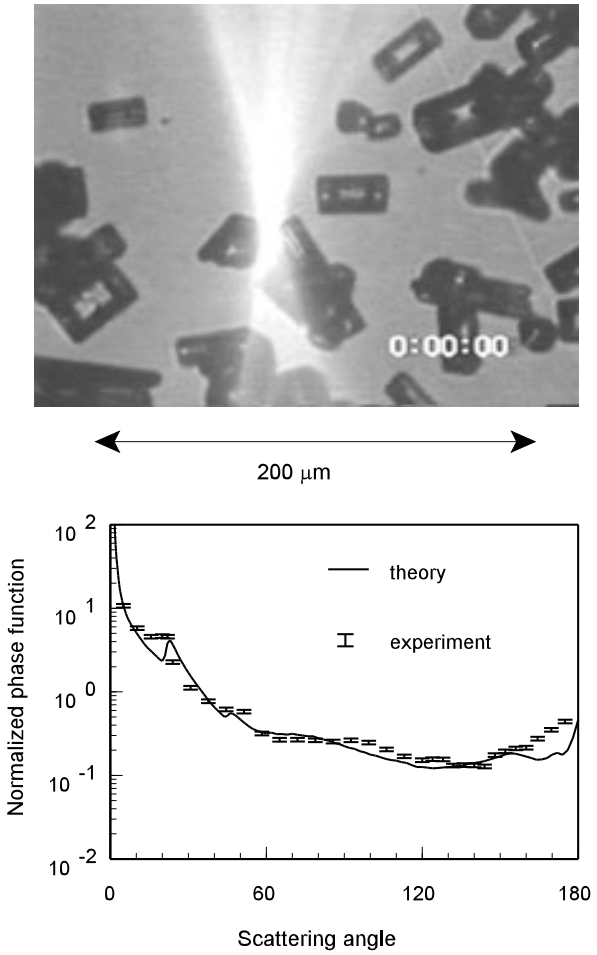

Fig.4. Same as Fig. 3, but for a cloud of column crystals.

caused by these limitations in determining the microphysical properties. In both cases, between 120° and 160° the experimental result is not smooth which is due to systematic errors in the calibration which are more noticeable at lower intensities. There is a slight difference between the angular position of both the 22° and 46° intensity peaks, because each fiber optic senses light scattered into an angle of about 2° and the angular positions of the fiber optics are not at the points of maximum scattered intensity.

5. SUMMARY

The light scattered by ice crystals into a 2D plane by two different and distinct cloud types, a cloud composed of plates and one composed of primarily hollow columns has been measured by a fiber optic based polar nephelometer. The microphysical properties of the cloud as determined by concurrent video microscope images are used to develop phase function expectations derived from geometric optics methods. Within the degree to which it is possible to determine the microphysical properties of the ice cloud, the expectation match the experimental result.

The presence of both the 22° and 46° intensity features, which are caused by refraction through the 60° and 90° prisms of the ice crystals are seen in the experimental results, and it is noted that the 46° feature is more prominent for the plate cloud, as is expected. In order to match the experimental result, a large percentage of the particles used in the expectation have rough surfaces, which could be due to either surface features on the particles which are not visible on the cloudscope and/or the presence of small particles which were not captured by the cloudscope.

The authors are grateful to Y. Takano for assistance in the theoretical interpretations presented in this paper. This research was supported by National Science Foundation Grant ATM-99-07924 and Air Force Office of Scientific Research Grant F49620-01-1-0057.

REFERENCES

Arnott, P., Y. Dong and J. Hallet, 1995: Extinction efficiency in the infrared (2-18μm) of laboratory ice clouds: observations of scattering minima in the Christiansen bands of ice, *Appl. Opt.*, **34,** 541 - 551.

Barkey, B., and K. N. Liou, 2000: Polar nephelometer for light scattering measurements of ice crystals, *Opt. Let.*, **26**, 232 - 234.

Liou, K. N., 1986: Influence of cirrus clouds on weather and climate processes: A global perspective, *Mon. Wea. Rev.,* **114,** 1167 - 1199.

Oshchepkov, S., I. Harumi, J. F. Gayet, A. Sinyuk, F. Auriol, and S. Havemann, 2000: Microphysical properties of mixed-phase and ice clouds retrieved from in situ airborne "polar nephelometer" measurements, *Geophys. Res. Lett.,* **27**, 209 - 212.

Pruppacher, H. R., and J. D. Klett, *Microphysics of Clouds and Radiation* Reidel, Dordrecht, the Netherlands, 1980, p. 40.

Takano, Y., and K. N. Liou, 1989: Solar radiative transfer in cirrus clouds. Part I:Single-scattering and optical properties of hexagonal ice crystals, *J. Atmos. Sci.*, **46**, 3 - 19.

Rolland, P., K. N. Liou, M. D. King, S. C. Tsay and G. M. McFarquhar, 2000: Remote sensing of optical and microphysical properties of cirrus clouds using Moderate-Resolution Imaging Spectroradiometer channels: methodology and sensitivity to physical assumptions, *J. Geophys. Res.,* **105**, 11721 -11738.

Yang, P., and K. N. Liou, 1996: A geometrics-optics/integral-equation method for light scattering by non-spherical ice crystals, *Appl. Opt.,* **35**, 6568 - 6584.